Quaternary Research 75 (2011) 11–17

Contents lists available at ScienceDirect

Quaternary Research

journal homepage: www.elsevier.com/locate/yqres

Short Paper

A signal-to-noise index to quantify the potential for peak detection in sediment–charcoal records

Ryan F. Kelly [a,*], Philip E. Higuera [b], Carolyn M. Barrett [c], Feng Sheng Hu [a,c]

[a] Department of Plant Biology, University of Illinois, Urbana, IL, USA
[b] Department of Forest Ecology and Biogeosciences, University of Idaho, Moscow, ID, USA
[c] Program in Ecology, Evolution, and Conservation Biology, University of Illinois, Urbana, IL, USA

ARTICLE INFO

Article history:
Received 4 March 2010
Available online 17 August 2010

Keywords:
Signal-to-noise index (SNI)
Charcoal analysis
Fire history
Lake sediment
Paleoecology

ABSTRACT

Charcoal peaks in lake-sediment records are commonly used to reconstruct fire histories spanning thousands of years, but quantitative methods for evaluating the suitability of records for peak detection are largely lacking. We present a signal-to-noise index (SNI) that quantifies the separation of charcoal peaks (signal) from other variability in a record (noise). We validate the SNI with simulated and empirical charcoal records and show that an SNI >3 consistently identifies records appropriate for peak detection. The SNI thus offers a means to evaluate the suitability of sediment–charcoal records for reconstructing local fires. MATLAB and R functions for calculating SNI are provided.

Published by Elsevier Inc. on behalf of University of Washington.

Introduction

Numerous fire-history studies have been published on the basis of the identification of peaks in lake-sediment records of macroscopic (typically >100 μm in diameter) charcoal (e.g., see reviews by Whitlock and Larsen (2001) and Gavin et al. (2007)). Analytical methods are typically based on a decomposition approach by which a time series of charcoal accumulation rates (CHAR) is detrended to isolate *background* and *peak* series (e.g., Clark et al., 1996; Long et al., 1998; Carcaillet et al., 2001; Gavin et al., 2006; Higuera et al., 2009). The background series represents long-term shifts in fire regimes (e.g., area burned, fuel characteristics) and taphonomic processes unrelated to fire occurrence (e.g., slope wash, sediment focusing), and it may be modeled with a variety of moving-average methods. Background CHAR is removed from the raw CHAR series by either subtraction or division to obtain a peak series, which is assumed to represent charcoal from local fires, plus random variability (i.e., noise). To separate the signal of local fires from noise, a threshold function is determined by one of several methods, and samples exceeding the threshold are interpreted as local fire episodes.

The decomposition approach has both theoretical (e.g., Clark, 1988; Higuera et al., 2007; Peters and Higuera, 2007) and empirical (e.g., Millspaugh and Whitlock, 1995; Gavin et al., 2003; Lynch et al., 2004; Higuera et al., 2010) support suggesting that in records from small lakes (< ~20 ha), identified peaks represent fires within ca. 500–1000 m of the sampling location. However, sediment–charcoal records are highly variable, both within and between sites (Power et al., 2008), and some records are clearly more appropriate for peak analysis than others. While a record with large peaks distinct from background values fits well within the conceptual framework outlined above, processes including sediment mixing or reduced sedimentation rates can create more ambiguous records (Higuera et al., 2007).

Despite broad adoption of the decomposition approach, methods for quantifying the suitability of a charcoal record for peak analysis were lacking prior to the recent introduction of a signal-to-noise index (SNI; Higuera et al., 2009). Here, we briefly review the rationale for such a metric and present an improved SNI with a stronger theoretical basis and more intuitive interpretation. We then validate the SNI through application to simulated charcoal records, a null model of random variability, and empirical records from Alaska, and we compare our new SNI to that introduced by Higuera et al. (2009). Our results indicate that SNI accurately reflects the prominence of CHAR peaks and therefore offers an important quantitative tool to improve the rigor of fire-history reconstructions from sediment–charcoal records.

Rationale and definition of a signal-to-noise index

Given a detrended CHAR time series (i.e., the peak series) and corresponding threshold (for an example, see Gavin et al. (2006) and Higuera et al. (2009)), the samples within a specified time window can be separated into two distinct populations: signal (S), containing those samples greater than the threshold, and noise (N), the remaining samples, which fall at or below the threshold (Figs. 1a and c). In practice, N follows a normal distribution reasonably well (e.g., as

* Corresponding author.
E-mail address: rkelly@life.illinois.edu (R.F. Kelly).

0033-5894/$ – see front matter. Published by Elsevier Inc. on behalf of University of Washington.
doi:10.1016/j.yqres.2010.07.011

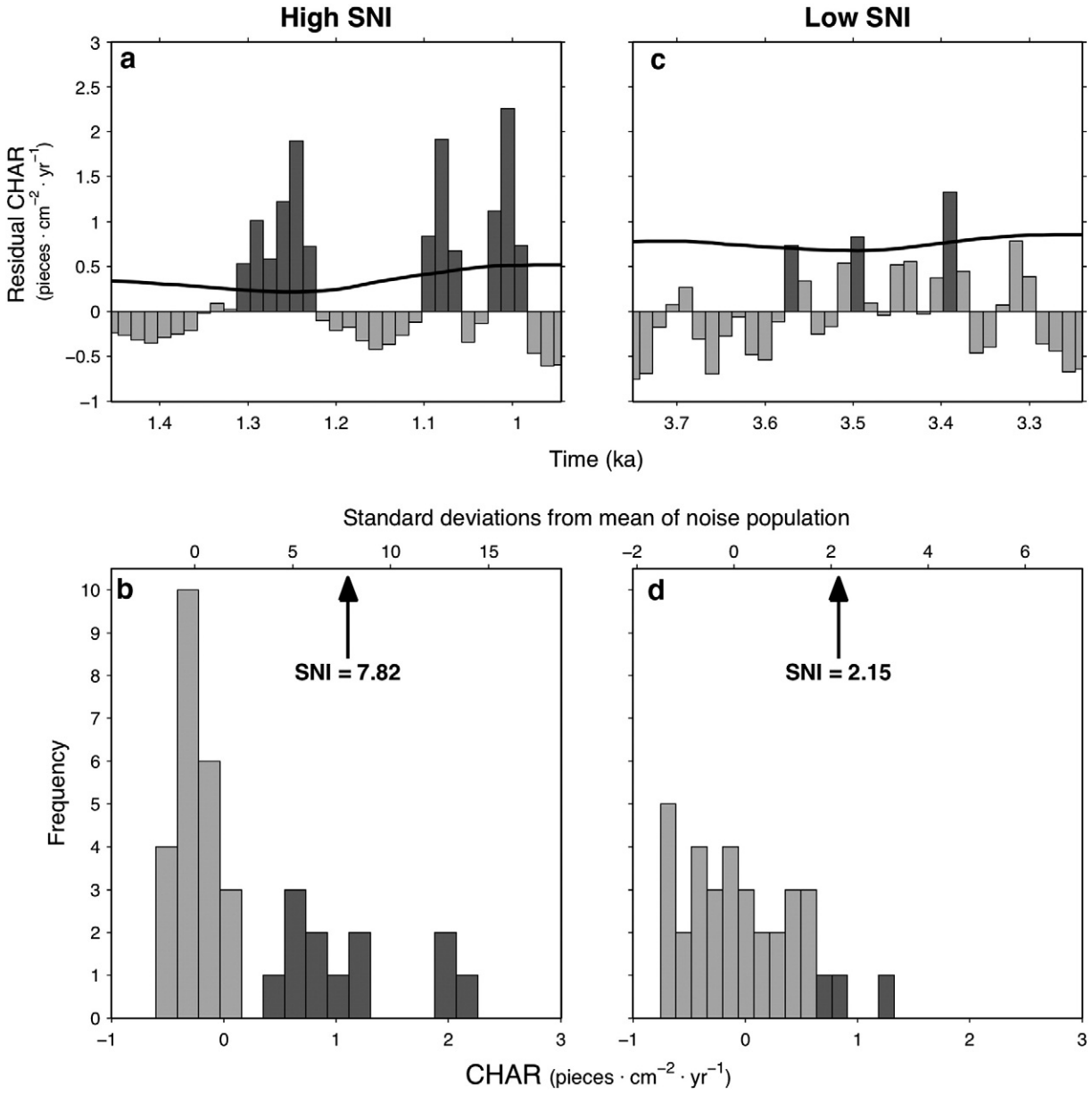

Figure 1. Illustration of SNI calculation (Eq. (2)) in single 500-yr windows from records CS1 (left) and CS3 (right). (a, c) Interpolated residual CHAR series separated into signal (*S*, dark bars) and noise (*N*, light bars) populations by a threshold (black line). (b, d) Histograms of CHAR values from (a) and (c), respectively, showing separation of *S* (dark bars) and *N* (light bars) for each. Top axis converts CHAR values into standard deviation units from the mean of *N*, and arrow indicates the mean of *S* on this axis, from which the proposed SNI is derived.

measured by a Lilliefors test), and we assume that noise is normally distributed in the following discussion.

Metrics for quantifying signal strength relative to accompanying noise are common in various fields (e.g., the signal-to-noise ratio used in image processing; Bankman, 2000), with formulation depending on the application. The SNI introduced by Higuera et al. (2009) compares the variability in the signal population, var(S), to the variability in the noise population, var(N):

$$SNI = \frac{\mathrm{var}(S)}{\mathrm{var}(S) + \mathrm{var}(N)} \quad (1)$$

In practice, when the signal and noise distributions are distinct, the variance of the signal distribution dominates the expression and $SNI \rightarrow 1$. This formulation implicitly assumes a positive relationship between the mean and variance of S, such that a signal distribution with a large (small) mean also has large (small) variance. While valid for many charcoal records, this assumption may not always hold. For example, a record could have a signal population distinct from the noise population, but with similar variance. In this scenario, an SNI of ~0.5 would under-represent the separation between signal and noise. Based on comparisons to a null model, Higuera et al. (2009) proposed that SNI>~0.5 is generally sufficient to warrant peak analysis.

Our aim in constructing a new SNI is to explicitly quantify the level of separation between S and N. There are numerous established methods for testing whether two samples arise from distinct distributions (e.g., the Kolmogorov–Smirnov test). However, since the use of a threshold implicitly separates S and N into non-overlapping populations, standard statistical tests are of little value, because they return very low p-values (typically $\ll 0.01$) regardless of

the apparent prominence of peaks in the record. The SNI presented below is conceptually based on such tests, but it produces a useful index reflecting the probability that the values in *S* could be drawn from the same population as *N*. Note that future work utilizing an SNI for charcoal records should reference this paper or Higuera et al. (2009) to distinguish the formula used; herein we refer to the SNI described below unless explicitly stated.

Specifically, given n_S samples in population *S* and n_N samples in population *N*, we define:

$$SNI = \begin{cases} \left(\frac{1}{n_s}\sum_{i=1}^{n_s}\frac{S_i-\overline{N}}{\sigma_N}\right)\left(\frac{n_N-2}{n_N}\right) & n_s \geq 1 \\ 0 & n_s = 0 \end{cases} \quad (2)$$

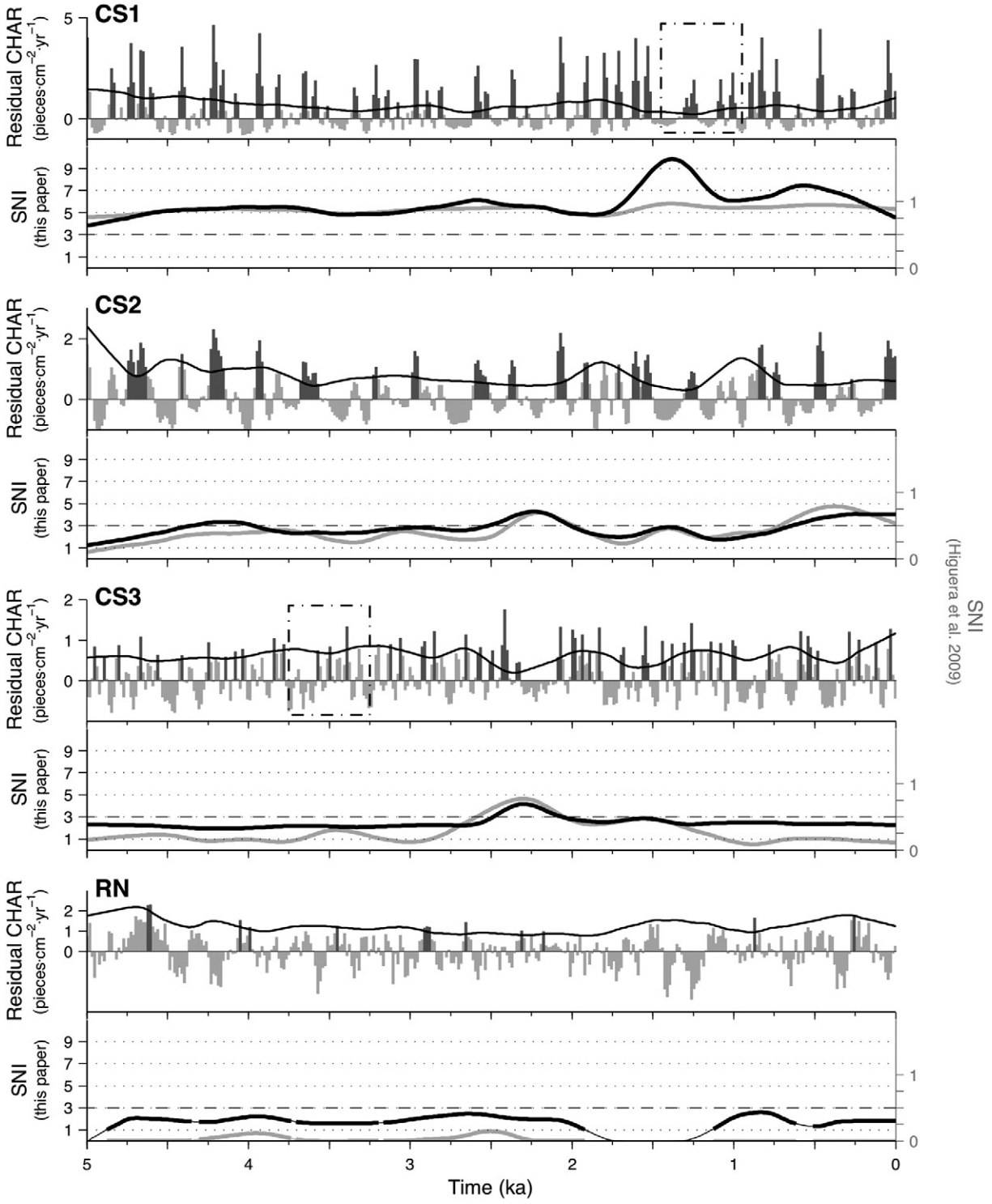

Figure 2. Comparison of SNI of four charcoal records: CS1, CS2, and CS3 are CharSim simulations, and RN is a null model of red noise. In each case, the upper panel shows signal (*S*, dark bars) and noise (*N*, light bars) samples in residual CHAR series, separated by a threshold (black line); dashed boxes indicate intervals illustrated in Figure 1. Lower panel shows SNI as defined by Higuera et al. (2009) (gray curve) and the new SNI presented here (black curve), and corresponding cutoff values for peak analysis (0.5 based on Higuera et al. and 3 based on this study; dashed line). Where no samples exceed the threshold within the SNI moving window, SNI is reduced by definition (thinned line in the bottom SNI plot; *see Eq. (2)*).

where $\{S_1, S_2, \ldots S_{n_s}\}$ are the CHAR values of individual samples in S, and $\overline{N}$ and σ_N are the mean and standard deviation, respectively, of the CHAR values in N. When no sample exceeds the threshold (i.e., $n_S = 0$), SNI = 0 by definition.

Eq. (2) leads to the convenient interpretation of SNI as the average separation of S and N, scaled by the standard deviation of N. The metric is thus analogous to the standard score (or "z-score") used commonly in statistics to quantify distance from the mean, and guidelines by which to interpret SNI values emerge from this likeness.

In a normal distribution, the 97.7th and 99.9th percentiles of observations fall two and three standard deviations above the mean, respectively. Thus, assuming a normally distributed noise component, this range (i.e., $[\overline{N} + 2\sigma_N] - [\overline{N} + 3\sigma_N]$) typically encompasses the largest values in N. Furthermore, since the noise and signal components are separated by definition, the same range represents a practical lower bound on S. It follows that SNI<3 (indicating that the samples of S are on average less than three standard deviations above the mean of N) occurs only when the two populations have little separation, that is when peaks are poorly defined relative to background (e.g., Figs. 1c and d). Conversely, SNI>3 results when S is relatively distinct from N (e.g., Figs. 1a and b). The range of SNI extends upward from this theoretical baseline without bound, reflecting ever greater separation between S and N. The factor of $(n_N - 2)/n_N$ in Eq. (2) is the ratio of the variance of the Student's t distribution with n_N degrees of freedom to that of the standard normal (Casella and Berger, 2002), and is included to account for bias due to the sample size of N.

Eq. (2) describes the SNI for signal and noise samples within a single time interval. This interval can span an entire record or some portion thereof. To compute SNI through time, individual SNI values are calculated for overlapping windows of a record, centered on each sample. The discrete steps of the moving window may result in sharp variations over adjacent time steps, which confound interpretation of the general temporal pattern of SNI. As a final step, therefore, a lowess smooth function (with window width equal to that used previously) is applied to obtain the final SNI series.

The choice of window width for computing and smoothing SNI depends somewhat subjectively on the time scale of interest. A relatively narrow window, for example, allows SNI to respond strongly to individual peaks in a charcoal record, but the small sample size within the window may undermine a robust assessment of overall signal quality. We suggest the natural choice of matching SNI window width to that used in computing background CHAR and/or the local threshold, and recommend exploring the sensitivity of this selection. Like any moving-window statistic, SNI is prone to edge effects (e.g., windows near the ends of the record encompass fewer samples), and thus we caution against over-interpreting trends in SNI near the ends of a record.

Data sources and quantitative analysis

To validate the SNI, we applied it to simulated charcoal records representing three hypothetical scenarios and to a null model of random variability (Fig. 2). Simulated records were generated using the CharSim model (Higuera et al., 2007), which simulates a spatially and temporally explicit fire regime, charcoal production and dispersal processes, primary (airborne) and secondary (slope wash and within-lake redeposition) deposition, sediment mixing, and sediment sampling. The CS1 scenario is based on model parameters representing boreal-forest charcoal records, with high temporal resolution (15-yr contiguous samples) and little vertical mixing in sediments. The CS2 scenario differs from CS1 only in that additional sediment mixing is simulated (vertical mixing depth doubled from 1.0 to 2.0 cm), as might be observed in shallower lakes. In both CS1 and CS2 scenarios, fire sizes mimic those observed in Alaska from 1988 to 2003 (Alaska Fire Service, 2004). By contrast, the CS3 scenario is based on fires of constant size, equal to the mean fire size of the same dataset. This scenario creates a charcoal series with a relatively uniform distribution of CHAR values, and illustrates a record in which peaks from local fires are difficult to detect due to processes independent of charcoal taphonomy. The null model record (RN) is a randomly generated series of red noise with mean, variance, and first-order autocorrelation comparable to empirical charcoal records described below. Similar to the use of red noise in other time series applications (e.g., wavelet analysis; Torrence and Compo, 1998), we assume that RN reflects properties of a time series that might arise by chance alone.

As a practical application, we also calculated SNI for four published charcoal records from Alaska. Sediment cores from Code (CO), Ruppert (RP), Wild Tussock (WK), and Xindi lakes (XI) in the south-central Brooks Range were analyzed for macroscopic charcoal content as described by Higuera et al. (2009). The records were interpolated to a constant 15-yr resolution before peak analysis.

For all records, peak analysis was based on the methods described by Higuera et al. (2009). Briefly, peak series were defined by subtracting background CHAR, modeled with a moving median or mode (as in the published records). Thresholds were determined using a Gaussian mixture model applied within a moving window ("local threshold"); at every time step, the assigned threshold value corresponds to the 99th percentile of the modeled noise distribution. We then calculated SNI for each record as described in the previous section. We used 500-yr windows for all moving-window procedures. For comparison, we also computed SNI based on the Higuera et al. (2009) formula (Eq. (1)). Finally, we calculated the SNI of RN using thresholds based on the 90th and 75th percentiles of the noise distribution identified by the mixture model (scenarios RN90 and RN75, respectively) to evaluate the sensitivity of SNI to threshold choice.

Results

The SNI of the simulated records varies in an intuitive way, and values >3 consistently identify records with distinct peaks. Among the simulated records, SNI values range from ~1 to 10 and exhibit low within-record variability (Fig. 2). The SNI of CS1 fluctuates around a median of 5.49 with a minimum of only 3.83. By contrast, CS2 and CS3 have lower SNI overall (median = 2.65 and 2.31, respectively), with values below the theoretical cutoff of 3.00 for the majority of each record.

The null model series has very low SNI, ranging from 0–2.60 with a median of 1.80 (Table 1; Fig. 2). Lowering the threshold in RN90 has a minor effect on SNI (median increases to 1.84), but all values remain below 3.00. The extremely low threshold in RN75 has a more

Table 1
Summary of SNI for all records.

Site	CO	RP	WK	XI, 15–5 cal ka BP	XI, 5–0 cal ka BP	CS1	CS2	CS3	RN	RN90	RN75
Median SNI	4.25	5.41	5.63	6.07	2.09	5.49	2.65	2.31	1.80	1.84	2.11
Min.–max. SNI	2.37–12.60	2.16–15.39	1.99–14.35	0.95–25.05	0.03–10.91	3.83–9.87	1.23–4.28	1.95–4.18	0.00–2.60	1.57–2.71	1.81–3.29
% of record with SNI>3	87	98	92	83	34	100	30	8	0	0	5

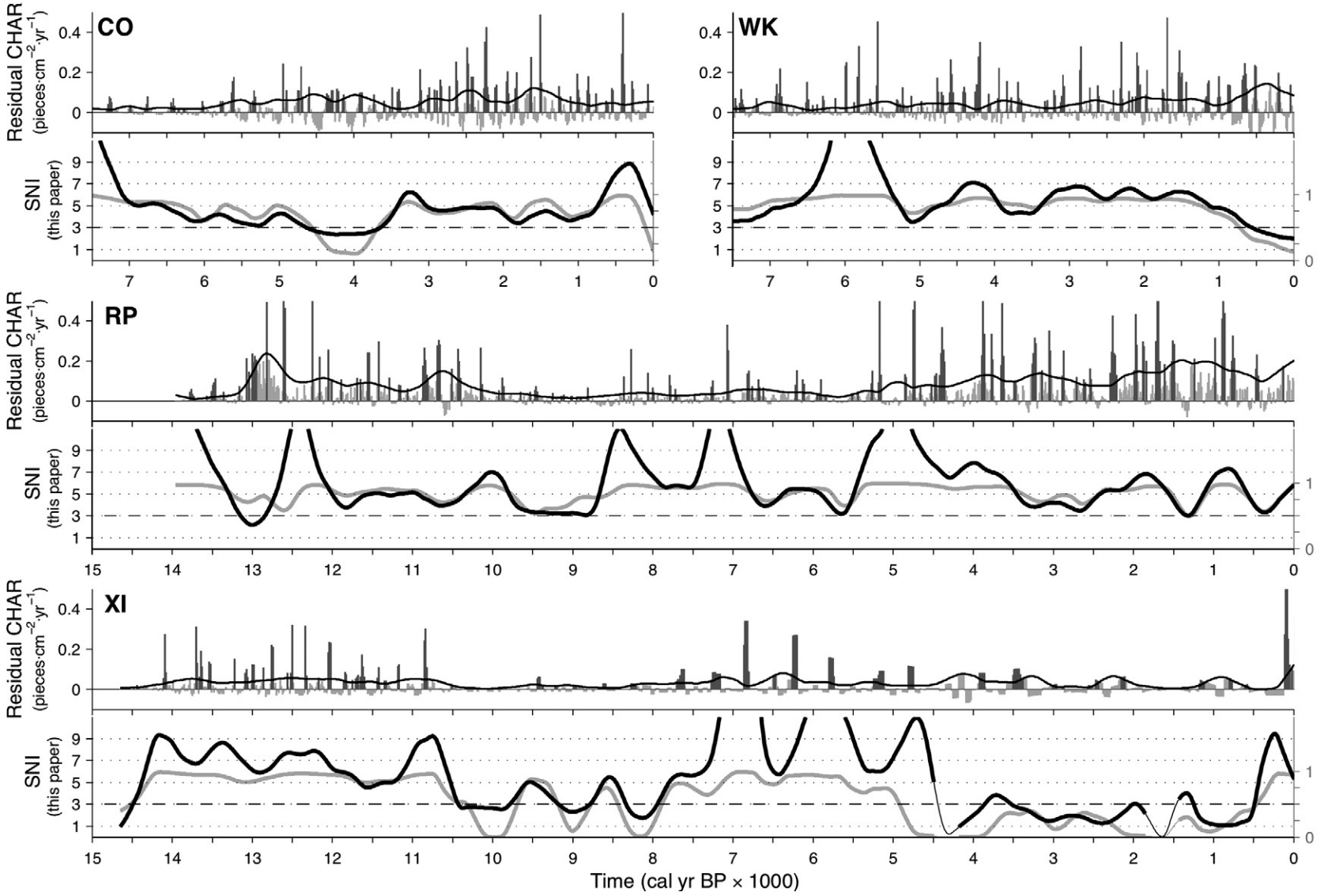

Figure 3. Comparison of SNI of empirical charcoal records obtained from lake-sediment cores in Alaska. Legend as in Figure 2.

pronounced effect (median SNI = 2.11), but still results in SNI < 3.00 for 95% of the record (Table 1, Fig. A1).

The empirical charcoal records show substantial variability in peak heights and SNI over time (Fig. 3). Nevertheless, the SNI at all sites is usually one to five times the theoretical cutoff of 3.00, corresponding to large, relatively distinct peaks. Instances of SNI < 3.00 occur in each record, but only intermittently for intervals of <1000 yr. Xindi Lake offers a notable exception, exhibiting an extended period of SNI < 3.00 after ca. 4.5 cal ka BP (Fig. 3). In both the simulated and empirical records, the two SNI metrics generally show similar patterns through time, although incongruent scales (in particular, the new SNI has no upper bound) preclude directly comparing the magnitude of their fluctuations (Figs. 2 and 3).

Discussion

The SNI introduced here is a promising means to quantify the suitability of charcoal records for peak analysis, and the theoretically-based cutoff of SNI = 3 works well to identify when peak identification is warranted. Applying this cutoff to a simulated high-resolution record (CS1) indicates a signal consistently well-separated from noise. By contrast, simulated records with taphonomic-related noise (CS2) or less-pronounced signals (CS3) result in SNI < 3, which cautions against inferring fire episodes from individual peaks. Equally important, low SNI successfully identifies our null model of random variability (RN) as clearly inappropriate for peak analysis (Fig. 2). The alternative threshold scenarios demonstrate that SNI is relatively insensitive to threshold choice, and minor changes to the threshold are unlikely to alter SNI interpretations (Table 1, Fig. A1).

When applied to empirical records, the SNI corroborates visual inspection and suggests a generally strong signal: all records except XI have SNI > 3 for at least 87% of the record (Table 1, Fig. 3). In some cases, however, empirical records have periods of SNI < ~3, suggesting that charcoal peaks during these intervals cannot be confidently separated from noise. In the case of XI, the period since ca. 4.5 cal ka BP was also identified as suspect with the SNI used by Higuera et al. (2009), and thus peaks in this period were not interpreted. For all records examined here, the two SNI formulas yield practically equivalent evaluations based on semi-independent reasoning. Thus, while we consider the new index a conceptual improvement, in practice both metrics quantify signal strength well.

Understanding why a record has a low SNI is important, because reduced SNI itself could have meaningful interpretations, depending on the causal mechanisms. Theoretically, a record can have a low SNI because of the lack of signal and/or the addition of noise. The latter mechanism is captured by CS2 (Fig. 2), where increased mixing diminishes the original signal and thus increases noise. The sediment mixing modeled in CS2 could arise from a number of natural processes, including wind-driven currents in shallow lakes, bioturbation, slow sediment accumulation, and/or low sample resolution. The empirical records XI and CO (Fig. 3) provide examples of reduced SNI due to these mechanisms. In XI, the low SNI after ca. 4.5 cal ka BP corresponds to decreased sediment accumulation rates, which, in combination with unchanging sample intervals of 0.5 cm, result in a resolution > 70 yr per sample (Higuera et al., 2009). This low sample resolution obscures the signal from large charcoal peaks, which are prominent in other portions of the record. Increased sediment mixing may explain the period of low SNI in Code Lake, ca. 4.5–3.5 cal ka BP.

Even in the absence of excessive noise, several mechanisms can contribute to low SNI in a charcoal record by obscuring the signal from local fires. The simulated record CS3 (Fig. 2) offers one such example. By dictating a constant, intermediate fire size in CharSim, we precluded the prominent signal (i.e., high CHAR values) that otherwise arises from large local fires. The result of dampened signal is accurately reflected in the low SNI of CS3. It is more difficult to find empirical examples where the signal from local fires is reduced, but such a scenario may result in ecosystems with low-severity fire regimes (Agee, 1993), where charcoal production per fire is low and varies little.

We conclude with two caveats regarding practical application of the proposed SNI. First, although the alternative threshold scenarios demonstrate the general robustness of SNI to threshold choice, they also highlight that SNI does not equate threshold credibility (e.g., RN75 uses an illogically low threshold but achieves a slightly higher SNI than the more reasonable RN). Thus, SNI cannot be used as a basis for threshold selection and must be strictly regarded as a *post hoc* tool for evaluating charcoal records with their thresholds determined *a priori*.

Second, it is important to note the distinction between SNI and the accuracy of charcoal analysis: SNI simply measures the separation between predefined *S* and *N* populations, whereas accuracy quantifies the tradeoff between identifying local fires and minimizing the number of false positives (e.g., Higuera et al., 2007). It is possible for a record to have low SNI when local fires are in fact correctly identified, or vice versa. For example, many peaks identified in CS3 actually do reflect simulated local fires, although the low SNI of the record indicates that these peaks cannot be confidently considered distinct from noise. Conversely, a record with distinct CHAR peaks from distant fires or non-fire processes (e.g., erosion events) might lead to low accuracy despite high SNI. With empirical records, of course, the true accuracy of peak identification is unknown, and thus it is paramount that analysts interpret SNI in the context of these possibilities, ideally substantiated with complementary data (e.g., sedimentological indicators of erosion). Insofar as the assumptions typical of sediment–charcoal analysis hold and the method for assigning the threshold is robust, such misleading instances should be rare.

Conclusions

The SNI metric introduced here provides a means to quantitatively assess whether charcoal records or portions thereof are appropriate for peak analysis. All charcoal records are influenced by multiple sources of variability, but many (including the majority of the empirical records shown here) nonetheless exhibit clear peaks. For these records, SNI simply offers quantitative support of subsequent peak analysis. Inevitably, however, some sediments yield more ambiguous charcoal series. In these cases, the cutoff value of SNI = 3 helps guard against over-interpretation of a weak signal, and fluctuations in SNI provide a means of interpreting temporal patterns in the noise itself. Thus, SNI is a valuable addition to the growing number of analytical tools aimed at quantifying fire history from sediment–charcoal records.

Acknowledgments

This analysis was supported by an NSF GK-12 Fellowship to RFK and NSF grant ARC 0612366 to FSH. The authors gratefully acknowledge advice from Michael Dietze, and thoughtful comments from Ben Clegg, Melissa Chipman, Hillary Lauren, Suzanne Nagi, and Michael Urban.

Appendix A. Supplementary material

Supplementary data associated with this article can be found, in the online version, at 10.1016/j.yqres.2010.07.011.

References

Agee, J.K., 1993. Fire Ecology of Pacific Northwest Forests. Island Press, Washington, DC.
Alaska Fire Service, 2004. Alaska Fire History. Bureau of Land Management. Bureau of Land Management. Alaska Fire Service.
Bankman, I.N., 2000. Handbook of Medical Imaging—Processing and Analysis. Academic Press.
Carcaillet, C., Bergeron, Y., Richard, P.J.H., Frechette, B., Gauthier, S., Prairie, Y.T., 2001. Change of fire frequency in the eastern Canadian boreal forests during the Holocene: does vegetation composition or climate trigger the fire regime? Journal of Ecology 89, 930–946.

Casella, G., Berger, R.L., 2002. Statistical Inference. Duxbury Press, Pacific Grove, CA.
Clark, J.S., 1988. Particle motion and the theory of charcoal analysis: source area, transport, deposition, and sampling. Quaternary Research 30, 67–80.
Clark, J.S., Royall, P.D., Chumbley, C., 1996. The role of fire during climate change in an eastern deciduous forest at Devil's Bathtub, New York. Ecology 77, 2148–2166.
Gavin, D.G., Brubaker, L.B., Lertzman, K.P., 2003. An 1800-year record of the spatial and temporal distribution of fire from the west coast of Vancouver Island, Canada. Canadian Journal of Forest Research 33, 573–586.
Gavin, D.G., Hallett, D.J., Hu, F.S., Lertzman, K.P., Prichard, S.J., Brown, K.J., Lynch, J.A., Bartlein, P., Peterson, D.L., 2007. Forest fire and climate change in western North America: insights from sediment charcoal records. Frontiers in Ecology and the Environment 5, 499–506.
Gavin, D.G., Hu, F.S., Lertzman, K., Corbett, P., 2006. Weak climatic control of stand-scale fire history during the late Holocene. Ecology 87, 1722–1732.
Higuera, P.E., Brubaker, L.B., Anderson, P.M., Hu, F.S., Brown, T.A., 2009. Vegetation mediated the impacts of postglacial climate change on fire regimes in the south-central Brooks Range, Alaska. Ecological Monographs 79, 201–219.
Higuera, P.E., Peters, M.E., Brubaker, L.B., Gavin, D.G., 2007. Understanding the origin and analysis of sediment–charcoal records with a simulation model. Quaternary Science Reviews 26, 1790–1809.
Higuera, P. E., Whitlock, C., Gage, J., 2010. Linking tree-ring and sediment–charcoal records to reconstruct fire occurrence and area burned in subalpine forests of Yellowstone National Park, U.S.A. The Holocene. doi:10.1177/0959683610374882.
Long, C.J., Whitlock, C., Bartlein, P.J., Millspaugh, S.H., 1998. A 9000-year fire history from the Oregon Coast Range, based on a high-resolution charcoal study. Canadian Journal of Forest Research 28, 774–787.
Lynch, J.A., Clark, J.S., Stocks, B.J., 2004. Charcoal production, dispersal and deposition from the Fort Providence experimental fire: interpreting fire regimes from charcoal records in boreal forests. Canadian Journal of Forest Research 34, 1642–1656.
Millspaugh, S.H., Whitlock, C., 1995. A 750-year fire history based on lake sediment records in central Yellowstone National Park, USA. Holocene 5, 283–292.
Peters, M.E., Higuera, P.E., 2007. Quantifying the source area of macroscopic charcoal with a particle dispersal model. Quaternary Research 67, 304–310.
Power, M.J., Marlon, J., Ortiz, N., Bartlein, P.J., Harrison, S.P., Mayle, F.E., Ballouche, A., Bradshaw, R.H.W., Carcaillet, C., Cordova, C., Mooney, S., Moreno, P.I., Prentice, I.C., Thonicke, K., Tinner, W., Whitlock, C., Zhang, Y., Zhao, Y., Ali, A.A., Anderson, R.S., Beer, R., Behling, H., Briles, C., Brown, K.J., Brunelle, A., Bush, M., Camill, P., Chu, G.Q., Clark, J., Colombaroli, D., Connor, S., Daniau, A.L., Daniels, M., Dodson, J., Doughty, E., Edwards, M.E., Finsinger, W., Foster, D., Frechette, J., Gaillard, M.J., Gavin, D.G., Gobet, E., Haberle, S., Hallett, D.J., Higuera, P., Hope, G., Horn, S., Inoue, J., Kaltenrieder, P., Kennedy, L., Kong, Z.C., Larsen, C., Long, C.J., Lynch, J., Lynch, E.A., McGlone, M., Meeks, S., Mensing, S., Meyer, G., Minckley, T., Mohr, J., Nelson, D.M., New, J., Newnham, R., Noti, R., Oswald, W., Pierce, J., Richard, P.J.H., Rowe, C., Goni, M.F.S., Shuman, B.N., Takahara, H., Toney, J., Turney, C., Urrego-Sanchez, D.H., Umbanhowar, C., Vandergoes, M., Vanniere, B., Vescovi, E., Walsh, M., Wang, X., Williams, N., Wilmshurst, J., Zhang, J.H., 2008. Changes in fire regimes since the Last Glacial Maximum: an assessment based on a global synthesis and analysis of charcoal data. Climate Dynamics 30, 887–907.
Torrence, C., Compo, G.P., 1998. A practical guide to wavelet analysis. Bulletin of the American Meteorological Society 79, 61–78.
Whitlock, C., Larsen, C., 2001. Charcoal as a fire proxy. *In* Tracking Environmental Change Using Lake Sediments. In: Smol, J.P., Birks, H.J.B., Last, W.M. (Eds.), Kluwer Academic Publisher, Dordrecht.